

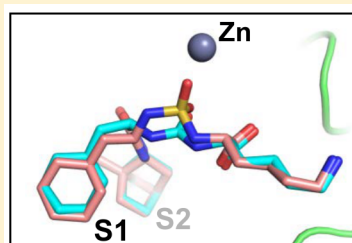
Sulfamide as Zinc Binding Motif in Small Molecule Inhibitors of Activated Thrombin Activatable Fibrinolysis Inhibitor (TAFIa)

Nis Halland,* Jörg Czech, Werngard Czechtizky, Andreas Evers, Markus Follmann,[†] Markus Kohlmann, Herman A. Schreuder, and Christopher Kallus*[‡]

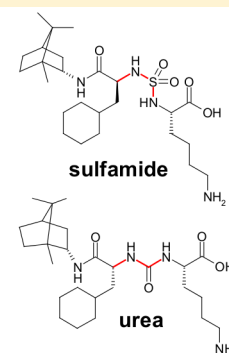
Sanofi R&D, Industriepark Höchst Building G838, D-65926 Frankfurt am Main, Germany

Supporting Information

ABSTRACT: Previously disclosed TAFIa inhibitors having a urea zinc-binding motif were used as the starting point for the development of a novel class of highly potent inhibitors having a sulfamide zinc-binding motif. High-resolution X-ray cocrystal structures were used to optimize the structures and reveal a highly unusual sulfamide configuration. A selected sulfamide was profiled in vitro and in vivo and displayed a promising ADMET profile.



stereochemistry matters in a new zinc binding mode for TAFI inhibitors



Antithrombotic agents usually act by preventing coagulation by targeting proteases such as thrombin, factor Xa, or factor VIIa in the coagulation cascade or by addressing antiplatelet targets like P2Y12 or GPVI.¹ An alternative approach would be to enhance fibrinolysis by targeting other downstream enzymes such as factor XIIIa or TAFIa. As TAFIa inhibition neither interferes with coagulation nor acts on platelet function or influences other thrombin actions, it is expected to present a novel antithrombotic mechanism with obvious advantages such as a low associated risk of bleeding.

TAFI, a 423 amino acid protein, is synthesized in the liver and present in plasma as a zymogen. When activated by thrombin by proteolysis at Arg92, activated TAFIa cleaves arginine and lysine residues on the surface of fibrin after initial plasmin degradation and is thus a part of the fine-tuned equilibrium of the coagulation–fibrinolysis system. By inhibition of TAFIa, plasmin formation and endogenous fibrinolysis are enhanced and an antithrombotic effect is achieved.^{2–7} TAFI, a member of the metalloprotease family, has a high selectivity for C-terminal basic amino acid side chains of proteins and peptides.^{8–10} The cleavage of the C-terminal peptide bond is catalyzed by coordination to a zinc ion present in the active site.¹¹

RESULTS AND DISCUSSION

We have recently reported the optimization of a relatively large anabaenopeptin natural product screening hit to a highly active small molecule TAFIa inhibitor.^{12–14} A common feature of these TAFIa inhibitors is the urea zinc binding motif where the urea carbonyl binds directly to the zinc atom in the metalloprotease. Early in our investigations we found the moderately active sulfamide screening hit **1** with $IC_{50} = 15 \mu M$.

We obtained an X-ray cocrystal structure of the complex. On the basis of this and a report by Ryu et al.¹⁵ where a sulfamide acts as zinc-binder in transition state analogue inhibitors of carboxypeptidase A, we speculated that we could expand the chemical space by replacing the urea zinc binder in our previously reported TAFIa inhibitors with a sulfamide moiety.¹⁶ To explore this unusual zinc binding motif, we prepared the direct sulfamide analogue of our previous lead structure (Figure 1) by the general synthesis route described in Scheme 1.

The key step in the synthesis of these analogues was performed by first converting the side chain protected basic amino acids to the corresponding N-sulfamidated oxazolidinones **2** using chlorosulfonyl isocyanate at 0 °C in CH_2Cl_2 (Scheme 1). These oxazolidinones underwent subsequent sulfamide formation by treatment with amino acid derivatives **4** in refluxing acetonitrile to afford the protected products **3**. Finally, the end products were obtained upon hydrogenolysis of the benzyl ester and Cbz group using 10% Pd/C in methanol at 1 bar hydrogen pressure.

The direct sulfamide analogue of the highly potent urea lead incorporating a (R)-configured cyclohexylalanine amino acid, **5a** (Figure 1) turned out to be a less potent TAFIa inhibitor with an IC_{50} of 75 μM , whereas the diastereoisomer **5b**, containing the (S)-configured cyclohexylalanine, showed a significantly higher inhibitory activity with an IC_{50} of 0.33 μM . In general, we found that the SAR of the sulfamide TAFI inhibitors was very similar to that of the urea series when the configuration of the nonbasic amino acid was changed from (R) to (S). The reason for this was not obvious even when

Received: August 26, 2016

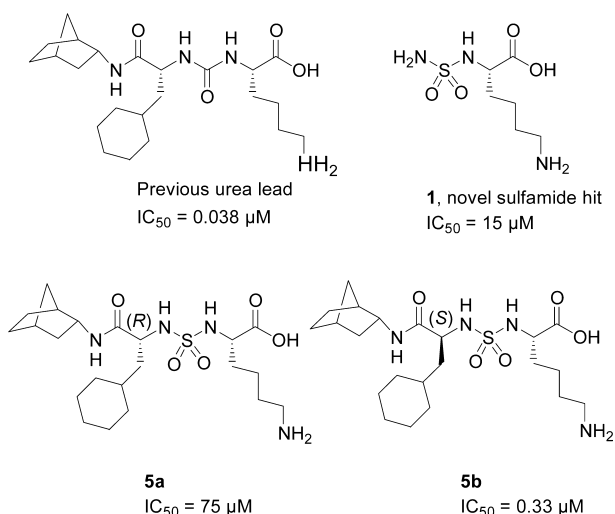
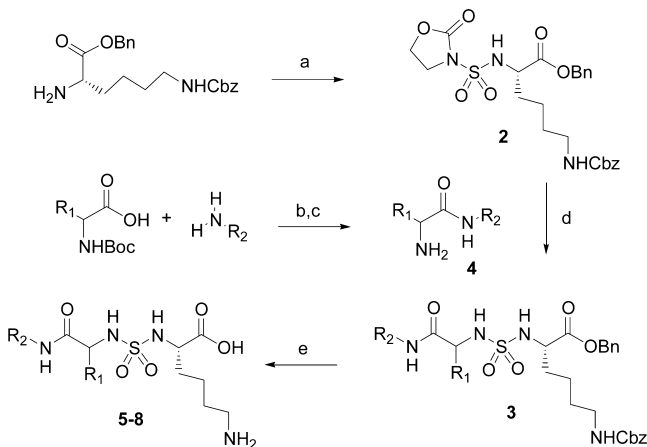


Figure 1. Sulfamide analogues 5a and 5b of the urea lead.

Scheme 1. Synthesis of Sulfamide TAFIa Inhibitors^a



^aReagents and conditions: (a) chlorosulfonyl isocyanate, 2-bromoethanol, triethylamine, CH₂Cl₂, 0 °C; (b) 1-hydroxybenzotriazole, 1-(3-dimethylaminopropyl)-3-ethylcarbodiimide hydrochloride, *N,N*-diisopropylethylamine, DMF, 20 °C; (c) TFA, CH₂Cl₂, 20 °C; (d) triethylamine, MeCN, 80 °C; (e) H₂ (1 bar), 10% Pd/C, MeOH, 20 °C.

considering the tetrahedral geometry of the sulfamide compared to the planar geometry of the urea. Intrigued by these results, we obtained X-ray cocrystal structures with various ligands bound to a surrogate enzyme to compare the two series. Due to the chemical instability of TAFIa, a “TAFInized” carboxypeptidase B (tafCPB) was used (see ref 12 and Supporting Information S2). We thus obtained high-resolution X-ray cocrystal structures of tafCPB complexed with two related analogues, either urea 9 (having an ((*R*)-configured cyclohexyl-alanine moiety) or sulfamide 7a with an ((*S*)-configured cyclohexylalanine moiety) (Figure 2). The structures showed that in both cocrystals the cyclohexyl rings and the norbornyl groups are nearly superimposable. Likewise, the amino and carboxy groups of the terminal lysine residues are almost superimposable. In both structures the ligand and enzyme are in the same configuration, and this is probably the reason for the similar activity observed (7a IC₅₀ = 12 nM; 9 IC₅₀ = 3 nM). The opposite configuration at the chiral carbon C* (adjacent to the sulfamide/urea moiety) was essential for

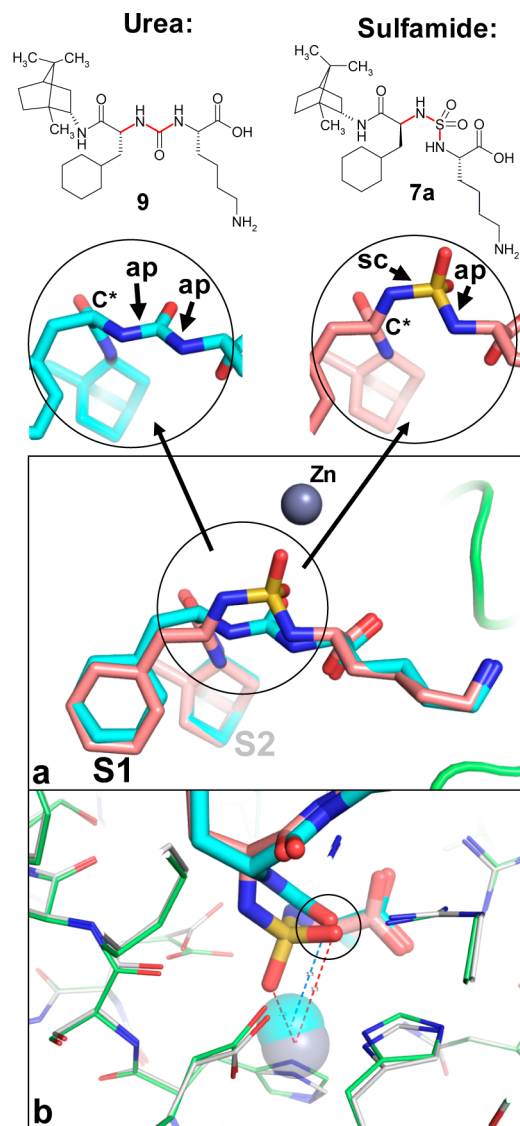


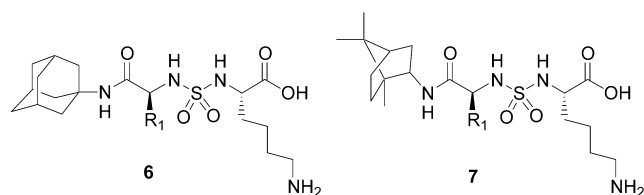
Figure 2. Superposition of the crystal structures of tafCPB with the urea inhibitor 9 (cyan; PDB code 4uib¹²) and the sulfamide inhibitor 7a (pink; PDB code 5lyi). (a) Overall view of the inhibitors. The arrows in the insets show the N(1)–S(O2) and N(1)–C(O) bonds with differing synclinal/antiperiplanar arrangements of the C* and N(2) residues. The bonds are indicated in red in the corresponding chemical structures. ap = antiperiplanar, sc = synclinal. (b) Close-up of the interactions of the urea/sulfamide oxygens with the catalytic zinc.

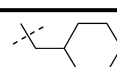
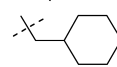
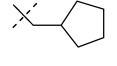
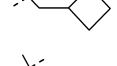
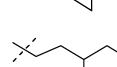
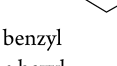
this highly similar arrangement: while 7a incorporated an (*S*)-configured carbon C* and a synclinal (sc) arrangement of C* and N(2) along the C*N(1)–S(O2)N(2) bond (indicated in red, Figure 2), the (*R*)-configured C* and the antiperiplanar (ap) arrangement of C* and N(2) along the C*N(1)–C(O)N(2) bond led to a similar spatial arrangement in 9. A search in the Cambridge Structural Database (CSD)¹⁷ for small-molecule crystal structures with symmetrical urea and sulfamide groups (excluding cyclic compounds) revealed a sharp antiperiplanar distribution with an average torsion angle of 173° for the urea compounds. In contrast, for sulfamides, a broader synclinal distribution centered around 61° (see Supporting Information S3) is found. No antiperiplanar torsion angles were found for the sulfamides, indicating that the antiperiplanar configuration along the second, adjacent SO₂–N(2) bond in Figure 2a must have been forced by the

complexation into the tafCBP active site, in line with the steep SAR we observed. The cocrystal structures showed that the catalytic zinc atom coordinated one of the two sulfamide oxygen atoms in the outer shell at a distance of 3.3 Å analogously to the coordination of the urea oxygen. Interestingly, the other sulfamide oxygen was located at 2.0 Å in the inner coordination shell of the catalytic zinc (Figure 2b).

The position of the zinc differs by 0.5 Å between the two structures, with the zinc from the **9** complex shown in cyan and the zinc from the **7a** complex in gray. Interestingly, the oxygen common between the urea and sulfamide complexes (circled) is at 3.3 Å in the outer coordination shell of the zinc, while the oxygen, unique to the sulfamide, is at 2.0 Å in the inner coordination shell. On the basis of these results, we attempted to improve the affinity. We prepared a small library, according to Scheme 1, of sulfamides having an (*S*) configuration at the nonbasic amino acid as in **5b**. First, the 1-adamantyl or (*R*)-(+)-bornyl amine groups of the terminal amide residue that were previously identified as yielding highly active TAFI inhibitors in the urea series were kept constant whereas the (*S*)-cyclohexylalanine amino acid moiety was systematically replaced by other (*S*)-configured amino acids with unfunctionalized side chains (Table 1).

Table 1. TAFIa Activity of Adamantylsulfamides **6** and (*R*)-(+)-Bornylsulfamides **7**: SAR of (*S*)-Cyclohexylalanine Amino Acid Replacements



	R1	IC ₅₀ (μM)
6a		0.49
6b	benzyl	2.1
6c	Ph	>30
6d	<i>i</i> -Pr	>30
6e	H	>30
6f	Me	>30
6g	<i>i</i> -Butyl	10
7a		0.012
7b		0.081
7c		0.36
7d		0.23
7e		0.22
7f	benzyl	0.17
7g	<i>c</i> -hexyl	47
7h	propyl	1.1
7i	ethyl	2.3

Replacement of the cyclohexylalanine amino acid by other amino acids with very small or no R1 side chains, e.g., alanine **6f** or glycine **6e** but also α -branched amino acid side chains such as **6d** or **6g**, led to less active compounds. Generally, medium-sized alkyl groups such as cyclopentylmethyl **7b**, cyclobutylmethyl **7c**, cyclopropylmethyl **7d**, propyl **7h**, or benzyl **7f** afforded very high TAFIa affinity, but none of them were as potent as the cyclohexylmethyl **7a** side chain.

From the X-ray cocrystal structures of **9** and **7a** it is observed that cyclohexylmethyl side chain has an almost perfect fit into a pocket in tafCPB rationalizing the high activity of **7a** and **9**. We observed that the (*R*)-(+)-bornylamides were usually more potent TAFIa inhibitors than the corresponding 1-adamantylamides. Consequently, the combination of the most active (*S*)-cyclohexylalanine amino acid with the (*R*)-(+)-bornylamide resulted in the very potent inhibitor **7a** with an IC₅₀ of 12 nM.

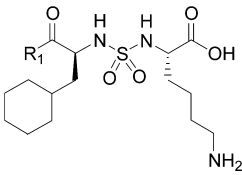
Turning our attention to exploring (*R*)-(+)-bornyl and 1-adamantyl replacements (R1), another small amide library was generated (Table 2). Replacing the bridged bornyl or adamantyl cycloalkanes by cyclohexyl or substituted cyclohexyl derivatives led to compounds with reduced activity, whereas the bicyclic amide **8f** showed an improved IC₅₀ of 0.67 μM compared to the less active monocyclic and acyclic residues. A number of additional amides incorporating bridged cycloalkanes generally showed a very high activity on TAFIa as exemplified by the (1*S*,2*S*,3*S*,5*R*)-(+)-isopinocampheylamide **8k** with an IC₅₀ of 0.13 μM.

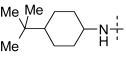
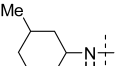
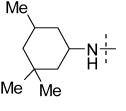
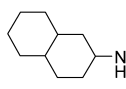
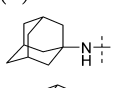
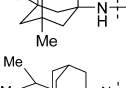
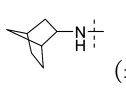
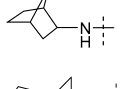
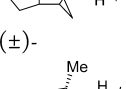
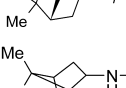
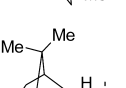
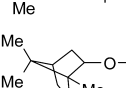
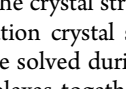
However, as in the urea series, the (*R*)-(+)-bornylamides still delivered the most potent TAFIa inhibitors indicating a similar binding mode. Interestingly, replacement of the (*R*)-(+)-bornylamide by a (*R*)-(+)-bornyl ester as in **8m** led to a more than 100-fold reduction in potency underlining the importance of the amide geometry and the presence of a hydrogen bond donor.

Keeping the (*R*)-(+)-bornylamide residue constant, we then replaced the lysine side chain by other amino acid residues and confirmed that a basic amino functionality is favorable for a high binding activity (Table 3).

For instance, replacing the lysine amino acid with a nonbasic phenylalanine as in **10c** furnished a less potent inhibitor with IC₅₀ = 24 μM. On the other hand, not all basic residues led to high binding affinity as exemplified by, for example, the *N*-dimethyl substituted lysine **10a**. Introduction of a nonbasic hydrogen bond donor such as OH in compound **10b**, an amide residue as in **10d**, or a urea as in **10f** also led to nearly inactive compounds. We therefore synthesized a number of sulfamides where the lysine was replaced by other amino acids containing less basic terminal groups such as aniline, imidazole, pyridine, or 2-aminopyridine residues (**10j–m**). All these compounds showed a good to excellent activity on TAFIa. Especially the 2-aminopyridine **10m** provided a highly active TAFI inhibitor with an IC₅₀ of 26 nM due to its ability make a bidentate interaction with Asp255. As seen from Table 3 some basic residues such as amidine (**10p**) or guanidine (**10q**) groups provided highly active TAFIa inhibitors in the low nanomolar range. Shortened linkers as in **10n** where the C4 lysine side chain was shortened to a C3 chain led to a reduction in activity as compared to **7a**. This is not surprising, since the natural TAFI substrates contain lysine or arginine residues and their respective C4 or C3 side chain is optimal for binding to the enzyme. A similar effect was observed when comparing **10o** and **10p**.

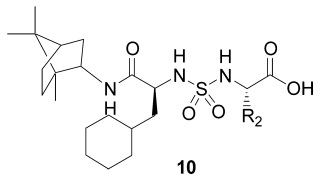
Table 2. TAFIa Binding Affinity of Sulfamides: SAR of Amide Substitution

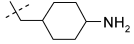
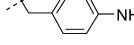
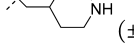
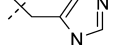
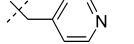
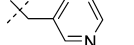
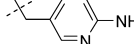
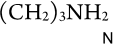
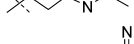


R1	IC ₅₀ (μM)
8a <i>t</i> -BuNH	6.7
8b <i>c</i> -Hex-NH	1.7
8c^a 	1.7
8d^a 	1.7
8e^a 	5.7
8f 	0.67
6a 	0.49
8g 	1.1
8h 	0.40
5b 	0.33
8i 	0.42
8j 	0.17
8k 	0.13
7a 	0.012
8l 	0.069
8m 	6.4

^aMixture of diastereomers.

Besides the crystal structure of 7a-tafCPB complex, two other high resolution crystal structures with the sulfamide ligands **1** and **6a** were solved during the optimization. A superposition of these complexes together with the urea **9** and the urea lead is

Table 3. TAFIa Activity of (*R*)-(+)-Bornylsulfamides **10** with Lysine Replacements


R2	IC ₅₀ (μM)
10a (CH ₂) ₄ NMe ₂	44
10b (CH ₂) ₄ OH	>30
10c CH ₂ Ph	24
10d (CH ₂) ₃ CONH ₂	>30
10e (CH ₂) ₄ NHAc	>30
10f (CH ₂) ₄ NHCONH ₂	>30
10g 	>30
10h 	7.1
10i 	0.88
10j 	4.4
10k 	1.7
10l 	0.2
10m 	0.026
10n (CH ₂) ₃ NH ₂	1.1
10o 	1.5
10p 	0.071
10q 	0.049

shown in Figure 3. Due to the high resolution (1.64–2.02 Å; see Figure S1 and Table S1), the atomic positions are accurately determined.

The coordinates of the inhibitors overlap almost perfectly, indicating that their binding modes are nearly identical. The only major difference observed, except for the differences due to the presence of a urea or sulfamide linker, is that the cyclohexyl group of the urea lead is rotated by 90° with respect to the cyclohexyl group of the other inhibitors. Stacked parallel to the aromatic ring of Tyr198, this orientation corresponds to the lower energy conformation. While this conformation is allowed by the compact norbornane group of **1**, this conformation is prohibited due to short contacts with the more bulky bornane and adamantane groups in the other inhibitors.

The hydrochloride salt of the potent sulfamide **7a** was selected for further in vitro eADMET and physicochemical profiling to assess its potential as preclinical candidate (Table 4). **7a** is a strong TAFI inhibitor with an IC₅₀ of 12 nM, and only a minor decrease in activity was observed in the presence of 1% human serum albumin. The activity in human pooled blood was also determined in a standard clot lysis assay and was

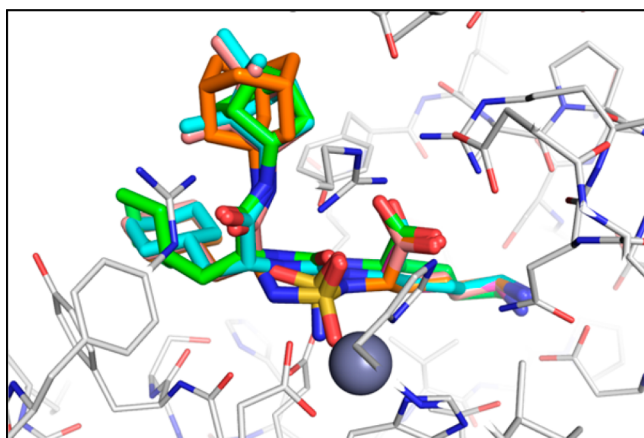


Figure 3. Superposition of the crystal structures of tafCPB with the urea lead (green, PDB code 5lyf) and sulfamides **1** (magenta, PDB code 5lyd), **7a** (pink, 5lyi), **6a** (orange, PDB code 5lyl), and **9** (cyan, PDB code 4uib). The protein part (white) is from the highest resolution structure with ligand **7a**.

Table 4. Physicochemical and in Vitro ADMET Properties of Sulfamide **7a**

property	value
MW (parent)	514.73
solubility mg/mL (pH 7.4, 25 °C)	0.457
log <i>D</i> (pH 7.4, 25 °C)	2.02
ClogP	4.52
PSA (Å ²)	159
H-bond donors	6
H-bond acceptors	9
rotatable bonds	12
LE (kcal/mol)/LLE	0.31/5.9
IC ₅₀ TAFIa (μM)	0.012
IC ₅₀ TAFIa (μM) + 1% human serum albumin	0.051
IC ₅₀ clot lysis assay (μM)	0.123
metabolic degradation in human microsomes (%) ^c	21
metabolic degradation in rat microsomes (%) ^c	8
metabolic degradation in mouse microsomes (%) ^c	0
intrinsic clearance in human hepatocytes ((mL/h)/10 ⁶ cells)	0.043
Caco2 permeability (×10 ⁻⁷ cm/s)	0.6 (low)
CYP3A4 inhibition IC ₅₀ (μM) midazolam site/testosterone site ^a	12/>30
CYP1A1, CYP1A2, CYP3A4 induction (%)	<10
hERG channel inhibition IC ₅₀ , patch clamp (μM) ^b	>10
other peptidases % inhibition at 100 μM FIIa, FVIIa, FXa, FXIa, FXIIa, urokinase, C 1s, tPA, trypsin, plasmin, KLKB1 ^d	<40

^aIncubated at 37 °C for 10–30 min at 0.3–30 μM. ^bPatch-clamp technique in the whole-cell configuration on recombinant chinese hamster ovary (CHO) cells. ^c% degradation after 20 min incubation (see Supporting Information for details). ^dKallikrein B, plasma (Fletcher factor) 1.

found to be high with IC₅₀ = 0.123 μM. The high activity of **7a** was also reflected by a ligand efficacy (LE) of 0.31 kcal/mol and high lipophilic ligand efficacy (LLE) of 5.9. **7a** is relatively polar with a log *D* of 2.0 and possesses a high aqueous solubility

(Table 4). Furthermore, **7a**, which was found to be stable when incubated with human, mouse, or rat microsomes, showed a very moderate intrinsic clearance in human hepatocytes and a moderate CYP3A4 inhibition with IC₅₀ = 12 μM at the midazolam binding site. **7a** did not display any CYP1A1, CYP1A2, or CYP3A4 induction or hERG channel liability. Lastly, **7a** was tested against a panel of other proteases at 100 μM and none of them were inhibited significantly. Altogether, **7a** displayed a very similar physicochemical and in vitro ADMET profile compared the corresponding urea **9**.¹² Due to the low Caco-2 permeability and high solubility, an intravenous application was considered the preferred route of administration for in vivo studies.

Compound **7a** was further profiled in an in vivo pharmacokinetic study in rat to determine pharmacokinetic parameters. After intravenous bolus administration of 1.0 mg/kg, blood and urine samples were collected for up to 24 h and the key pharmacokinetic parameters determined (Table 5). The

Table 5. Pharmacokinetic Parameters of **7a** in Rat after Intravenous Bolus Administration of 1 mg/kg

parameter	
<i>t</i> _{1/2} (h)	1.7
<i>C</i> ₀ (ng/mL)	3800
clearance (L h ⁻¹ kg ⁻¹)	0.70
<i>V</i> _{ss} (L/kg)	0.38
% of dose excreted into urine after 24 h	4

compound is cleared relatively rapidly in rat with a terminal half-life of 1.7 h, and 4% of the administered dose is excreted into urine after 24 h. The volume of distribution at steady state was calculated to be 0.38 L/kg with plasma concentrations above IC₅₀ for up to 4 h after administration but below detectable levels after 24 h. Overall, this profile is compatible with administration by iv infusion in the clinic as the relative short half-life quickly leads to steady state plasma concentrations and enables a quick washout of the drug after treatment has ended.

CONCLUSION

In summary, we have developed a novel class of small molecule TAFIa inhibitors using a sulfamide moiety as an unusual zinc binding motif. X-ray cocrystal structures elucidated the specific interactions between ligand and enzyme. A series of sulfamides exhibit a similar SAR compared to our previously reported urea series when the configuration of one chiral center was reversed. Further cocrystal structures were obtained to clarify this unexpected result and revealed that this was due to a highly unusual sulfamide configuration that allowed the same spatial occupancy. The highly active sulfamide **7a** displays an attractive in vitro ADMET and in vivo PK profile suitable for further in vivo efficacy studies.

EXPERIMENTAL SECTION

X-ray Crystal Structure Determination. A mutated “tafinized” porcine carboxypeptidase B (T111-L416; SwissProt sequence) was used where 8 residues, closest to the active site that were different between CPB and TAFI, were mutated to their TAFI equivalents. These mutations were F175I, T302S, M309H, L311V, I355L, P357L, A359P, and S362G. The recombinant protein was expressed in *P. pastoris* GS115. The purified protein was dissolved in 50 mM Tris-HCl, pH 7.5, and concentrated to 11 mg/mL. 1 μL of protein solution was equilibrated against 1 μL of reservoir solutions containing 16–20%

PEG3350, 100 mM MES, pH 5.5, and 50 mM Zn acetate. Crystals were soaked with inhibitors by adding 1 μ L of a 10 mM solution of inhibitor in DMSO to a CPB crystal in 9 μ L of reservoir solution. After overnight incubation, the crystal was transferred to a drop of 8 μ L of soakbuffer with 2 μ L of glycerol and the crystal was picked with a nylon loop and flash frozen in liquid nitrogen. Data were collected at the European Synchrotron Radiation Facility (ESRF). Data processing and scaling were carried out using the XDS package. Model building and inhibitor fitting was done with Quanta and Coot, and refinement was done with Buster (1) and Refmac (urea lead and 7a and 8a). The crystals diffracted to between 1.64 and 2.02 Å resolution with an overall R_{meas} between 7.1% and 11.0% (see Table S1). The resulting maps were of excellent quality and clearly and unambiguously revealed the binding modes of the inhibitors (see Figure S1).

Chemistry. ^1H NMR spectra were recorded in the indicated deuterated solvent at 400 or 500 MHz. Purity of all compounds tested in biological assays were determined to be >95% by LCMS.

All sulfamides were prepared following the procedure for ((S)-6-amino-2-[[[(S)-2-cyclohexyl-1-((1R,2S,4R)-1,7,7-trimethylbicyclo[2.2.1]hept-2-ylcarbonyl)ethylsulfamidyl]]hexanoic acid 7a

(S)-6-Benzoyloxycarbonylamino-2(2-oxo-oxazolidine-sulfonylamino)hexanoic Acid Benzyl Ester (2). To a solution of 5.21 g of chlorosulfonyl isocyanate (36.9 mmol, 1.0 equiv) in dichloromethane (300 mL) under argon at 0 °C was slowly added a solution of 2.61 mL of 2-bromoethanol (36.9 mmol, 1.0 equiv) in dichloromethane (20 mL) at a rate so that the internal temperature was kept below 10 °C. After addition the reaction mixture was allowed to stir for an additional 30 min at 0 °C. To this solution was dropwise added a mixture of 15.00 g of H-Lys(Z)-OBzL·HCl (36.9 mmol, 1.0 equiv) and 16.5 mL of triethylamine (118.0 mmol, 3.2 equiv) in 120 mL of CH_2Cl_2 , keeping the temperature of the reaction mixture below 10 °C. After addition the ice bath was removed and the mixture stirred at ambient temperature for 4 h. Then the reaction mixture was washed three times with 100 mL of 0.2 M HCl (aq), dried over Na_2SO_4 , and evaporated to afford 18.4 g of the crude title compound 2 as a colorless oil that was used directly in the next step. ^1H NMR (DMSO- d_6 , 500 MHz) δ 1.24–1.44 (m, 4H), 1.54–1.63 (m, 1H), 1.68–1.77 (m, 1H), 2.95 (q, 2H, $J = 6.5$ Hz), 3.85 (q, 1H, $J = 7.8$ Hz), 3.94 (q, 1H, $J = 8.6$ Hz), 4.08–4.14 (m, 1H), 4.27 (t, 2H, $J = 8.2$ Hz), 5.00 (s, 2H), 5.12 (s, 2H), 7.18–7.25 (m, 1H), 7.27–7.42 (m, 10H), 9.05 (d, 1H, $J = 8.4$ Hz). MS (ES+) calcd: [M + H] 520.17. Found: 520.30.

(S)-6-Benzoyloxycarbonylamino-2-[[[(S)-2-cyclohexyl-1-((1R,2S,4R)-1,7,7-trimethylbicyclo[2.2.1]hept-2-ylcarbonyl)ethylsulfamidyl]]hexanoic Acid Benzyl Ester (3a). To a solution of 6.5 g of [(S)-2-cyclohexyl-1-((1R,2S,4R)-1,7,7-trimethylbicyclo[2.2.1]hept-2-ylcarbonyl)ethyl]carbamic acid *tert*-butyl ester 4a (16.0 mmol) in 50 mL of CH_2Cl_2 under argon at 0 °C was slowly added 50 mL of TFA, and the reaction was allowed to warm to ambient temperature. After 3 h the reaction mixture was evaporated to remove excess TFA and CH_2Cl_2 to afford 4.9 g of crude (S)-2-amino-3-cyclohexyl-*N*-((1R,2S,4R)-1,7,7-trimethylbicyclo[2.2.1]hept-2-yl)propionamide trifluoroacetic acid salt (16.0 mmol, 1.0 equiv) as a slightly yellow oil that was dissolved in MeCN (80 mL), and 8.9 mL of Et_3N was added together with 11.63 g of (S)-6-benzoyloxycarbonylamino-2(2-oxo-oxazolidinesulfonylamino)hexanoic acid benzyl ester 2 (22.4 mmol, 1.4 equiv). The reaction mixture was heated to reflux for 20 h. After cooling, the volatiles were evaporated and the crude reaction mixture was purified directly by flash chromatography using silica gel as the stationary phase and heptane/EtOAc as the eluent. This afforded 9.0 g (76% yield) of (S)-6-benzoyloxycarbonylamino-2-[[[(S)-2-cyclohexyl-1-((1R,2S,4R)-1,7,7-trimethylbicyclo[2.2.1]hept-2-ylcarbonyl)ethylsulfamidyl]]hexanoic acid benzyl ester 3a as a colorless foam after evaporation. ^1H NMR (DMSO- d_6 , 500 MHz) δ 0.68 (s, 3H), 0.79–0.92 (m, 3H), 0.81 (s, 3H) 0.86, (s, 3H), 1.05–1.43 (m, 12H), 1.37, 1.53–1.79 (m, 10H), 2.06–2.15 (m, 1H), 2.93 (q, 2H, $J = 6.4$ Hz), 3.73–3.83 (m, 2H), 4.08 (m, 1H), 4.99 (s, 2H), 5.12 (d, 2H, $J = 5.2$ Hz), 6.96 (d, 1H, $J = 8.9$ Hz), 7.18–7.22 (m, 2H), 7.28–7.41 (m, 10H), 7.64 (d, 1H, $J = 8.8$ Hz). MS (ES+) calcd: [M + H] 739.41. Found: 739.43.

[(S)-2-Cyclohexyl-1-((1R,2S,4R)-1,7,7-trimethylbicyclo[2.2.1]hept-2-ylcarbonyl)ethyl]carbamic Acid *tert*-Butyl Ester (4a).

To a solution of 5.0 g of (S)-2-*tert*-butoxycarbonylamino-3-cyclohexylpropionic acid (Boc-Cha-OH, 18.4 mmol, 1.0 equiv) in DMF (60 mL) under argon at 0 °C were added 3.53 g of 1-ethyl-3-(3-dimethylaminopropyl)carbodiimide hydrochloride (18.4 mmol, 1.0 equiv), 1.25 g of 1-hydroxybenzotriazole (9.2 mmol, 0.5 equiv), and 7.3 mL of Hünig's base, and the mixture was stirred for 30 min. Then 2.83 g of (R)-(+)-bornylamine (18.4 mmol, 1.0 equiv) and 3.7 mL of Hünig's base were added and the reaction was stirred for 16 h at ambient temperature. The reaction mixture was quenched with NaHCO_3 (sat., aq) and extracted with EtOAc three times. The combined organic phases were washed with water two times and dried over Na_2SO_4 before evaporation. Purification by flash chromatography using silica gel as the stationary phase and heptane/EtOAc as the eluent afforded 6.58 g (88% yield) of the title compound as a colorless solid. ^1H NMR (DMSO- d_6 , 500 MHz) δ 0.65 (s, 3H), 0.80–0.91 (m, 3H), 0.82 (s, 3H) 0.89, (s, 3H), 1.06–1.41 (m, 7H), 1.37 (s, 9H), 1.56–1.74 (m, 8H), 2.06–2.16 (m, 1H), 4.02 (q, 2H, $J = 7.6$ Hz), 4.09 (m, 1H), 6.67 (d, 1H, $J = 8.1$ Hz), 7.56 (d, 1H, $J = 8.6$ Hz). MS (ES+) calcd: [M + H] 407.33. Found: 407.32.

(S)-6-Amino-2-[[[(S)-2-cyclohexyl-1-((1R,2S,4R)-1,7,7-trimethylbicyclo[2.2.1]hept-2-ylcarbonyl)ethylsulfamidyl]]hexanoic Acid (7a).

9.0 g of (S)-6-benzoyloxycarbonylamino-2-[[[(S)-2-cyclohexyl-1-((1R,2S,4R)-1,7,7-trimethylbicyclo[2.2.1]hept-2-ylcarbonyl)ethylsulfamidyl]]hexanoic acid benzyl ester 3a (12.2 mmol) was dissolved in 90 mL of methanol, 600 mg of 10% Pd/C was added, and the reaction flask was kept under a hydrogen atmosphere at ambient temperature and pressure and stirred for 3.5 h. The reaction mixture was then filtered using Celite filter aid and evaporated under vacuum to afford 6.1 g (97%) of the title compound as a colorless oil. The product was dissolved in MeCN and water was added to afford a suspension in a 1:10 MeCN/water mixture. The solvents were removed by freeze-drying to afford the title compound as a colorless solid. ^1H NMR (DMSO- d_6 , 500 MHz) δ 0.68 (s, 3H), 0.82 (s, 3H), 0.83–0.91 (m, 2H), 0.89 (s, 3H), 0.97 (dd, 1H, $J = 4.8, 13.0$ Hz), 1.08–1.34 (m, 7H), 1.35–1.55 (m, 5H), 1.56–1.72 (m, 9H), 1.78 (d, 1H, $J = 13.0$ Hz), 2.04–2.13 (m, 1H), 2.75 (t, 2H, $J = 7.1$ Hz), 3.51 (t, 1H, $J = 5.5$ Hz), 3.83 (t, 1H, $J = 7.0$ Hz), 4.03–4.10 (m, 1H), 6.91–7.05 (br, 1H), 7.77 (d, 1H, $J = 8.8$ Hz), 7.5–8.2 (br, 2H). MS (ES+) calcd: [M + H] 515.33. Found: 515.35.

■ ASSOCIATED CONTENT

Supporting Information

The Supporting Information is available free of charge on the ACS Publications website at DOI: 10.1021/acs.jmedchem.6b01276.

Representative experimental procedures for X-ray crystallography, synthesis, biochemical assays, and analytical data for all compounds (PDF)

Molecular formula strings and some data (CSV)

Accession Codes

Atomic coordinates and structure factors for the urea lead and compounds 1, 6a, and 7a can be accessed using PDB codes Slyf, Slyd, Slyl, and Slyi, respectively. The authors will release the atomic coordinates and experimental data upon article publication.

■ AUTHOR INFORMATION

Corresponding Authors

*N.H.: phone, +49-69305-36193; e-mail, Nis.Halland@sanofi.com.

*C.K.: phone, +49-69305-34322; e-mail, christopher.kallus@bayer.com.

Present Addresses

†M.F.: Bayer Pharma AG, Aprather Weg 18A, D-42113 Wuppertal, Germany.

‡C.K.: Bayer Cropscience, Industriepark Höchst Building G836, D-65926 Frankfurt am Main, Germany.

Notes

The authors declare no competing financial interest.

ACKNOWLEDGMENTS

The authors thank Stefan Dierl and Britta Böhnisch for the preparation of tafinized CPB, and Alexander Liesum and Petra Loenze for growing the crystals and help with data processing and refinement.

REFERENCES

- (1) Gresele, P.; Agnelli, G. Novel approaches to the treatment of thrombosis. *Trends Pharmacol. Sci.* **2002**, *23*, 25–32.
- (2) Bajzar, L.; Manuel, R.; Nesheim, M. E. Purification and characterization of TAFI, a thrombin-activable fibrinolysis inhibitor. *J. Biol. Chem.* **1995**, *270*, 14477–14484.
- (3) Bouma, B. N.; Meijers, J. C. M. Thrombin-activatable fibrinolysis inhibitor (TAFI, plasma procarboxypeptidase B, procarboxypeptidase R, procarboxypeptidase U). *J. Thromb. Haemostasis* **2003**, *1*, 1566–1574.
- (4) Vercauteren, E.; Gils, A.; Declerck, P. J. Thrombin activatable fibrinolysis inhibitor: a putative target to enhance fibrinolysis. *Semin. Thromb. Hemostasis* **2013**, *39* (4), 365–372.
- (5) Fernandez, D.; Pallares, I.; Covaleda, G.; Aviles, F. X.; Vendrell, J. Metalloproteases and their inhibitors: recent developments in biomedically relevant protein and organic ligands. *Curr. Med. Chem.* **2013**, *20*, 1595–1608.
- (6) Willemse, J. L.; Heylen, E.; Nesheim, M. E.; Hendriks, D. F. Carboxypeptidase U (TAFIa): a new drug target for fibrinolytic therapy? *J. Thromb. Haemostasis* **2009**, *7*, 1962–1971.
- (7) Vercauteren, E.; Peeters, M.; Hoylaerts, M. F.; Lijnen, H. R.; Meijers, J. C. M.; Declerck, P. J.; Gils, A. The hyperfibrinolytic state of mice with combined thrombin-activatable fibrinolysis (TAFI) and plasminogen activator inhibitor -1 gene deficiency is critically dependent on TAFI deficiency. *J. Thromb. Haemostasis* **2012**, *10*, 2555–2562.
- (8) Hendriks, D.; Scharpé, S.; van Sande, M.; Lommaert, M. P. Characterisation of a carboxypeptidase in human serum distinct from carboxypeptidase N. *Clin. Chem. Lab. Med.* **1989**, *27*, 277–285.
- (9) Campbell, W.; Okada, H. An arginine specific carboxypeptidase generated in blood during coagulation or inflammation which is unrelated to carboxypeptidase N or its subunits. *Biochem. Biophys. Res. Commun.* **1989**, *162*, 933–939.
- (10) Tan, A. K.; Eaton, D. L. Activation and characterization of procarboxypeptidase B from human plasma. *Biochemistry* **1995**, *34*, 5811–5816.
- (11) Christianson, D. W.; Lipscomb, W. N. Carboxypeptidase A. *Acc. Chem. Res.* **1989**, *22*, 62–69.
- (12) Halland, N.; Brønstrup, M.; Czech, J.; Czechtizky, W.; Evers, A.; Follmann, M.; Kohlmann, M.; Schiell, M.; Kurz, M.; Schreuder, H. A.; Kallus, C. Novel small molecule inhibitors of activated thrombin activatable fibrinolysis inhibitor (TAFIa) from natural product Anabaenopeptin. *J. Med. Chem.* **2015**, *58*, 4839–4844.
- (13) Kallus, C.; Broenstrup, M.; Czechtizky, W.; Evers, A.; Follmann, M.; Halland, N.; Schreuder, H. Urea and sulfamide derivatives as TAFIa inhibitors. WO 2008067909, 2008.
- (14) Schreuder, H.; Liesum, A.; Lönze, P.; Stump, H.; Hoffmann, H.; Schiell, M.; Kurz, M.; Toti, L.; Bauer, A.; Kallus, C.; Klemke-Jahn, C.; Czech, J.; Kramer, D.; Enke, H.; Niedermeyer, T. H. J.; Morrison, V.; Kumar, V.; Brønstrup, M. Isolation, co-crystallization and structure-based characterization of anabaenopeptins as highly potent inhibitors of activated thrombin activatable fibrinolysis inhibitor (TAFIa). *Sci. Rep.* **2016**, *6*, 32958.
- (15) Park, J. D.; Kim, D. H.; Kim, S.-J.; Woo, J.-R.; Ryu, S. E. Sulfamide-based inhibitors for carboxypeptidase A. Novel type transition state analogue inhibitors for zinc proteases. *J. Med. Chem.* **2002**, *45*, 5295–5302.
- (16) Akparov, V.; Sokolenko, N.; Timofeev, V.; Kuranova, I. Structure of the complex of carboxypeptidase B and N-sulfamoyl-L-arginine. *Acta Crystallogr., Sect. F: Struct. Biol. Commun.* **2015**, *71*, 1335–1340.
- (17) Allen, F. H. The Cambridge Structural Database: a quarter of a million crystal structures and rising. *Acta Crystallogr., Sect. B: Struct. Sci.* **2002**, *58*, 380–388.